Received: 22 April 2021 | Revised: 23 July 2021 | Accepted: 27 July 2021

DOI: 10.1111/jne.13021

ORIGINAL ARTICLE

Journal of Neuroendocrinology WILEY

Morphological assessment of GABA and glutamate inputs to GnRH neurons in intact female mice using expansion microscopy

Shel-Hwa Yeo[1,2] | Michel K. Herde[1] | Allan E. Herbison[1,2]

[1]Centre for Neuroendocrinology and Department of Physiology, School of Biomedical Sciences, University of Otago, Dunedin, New Zealand

[2]Department of Physiology Development and Neuroscience, University of Cambridge, Cambridge, UK

Correspondence
Allan E. Herbison, Department of Physiology, Development and Neuroscience, University of Cambridge, Cambridge CB2 3EG, UK.
Email: aeh36@cam.ac.uk

Funding information
Wellcome Trust; Health Research Council of New Zealand

Abstract

The roles GABAergic and glutamatergic inputs in regulating the activity of the gonadotrophin-releasing hormone (GnRH) neurons at the time of the preovulatory surge remain unclear. We used expansion microscopy to compare the density of GABAergic and glutamatergic synapses on the GnRH neuron cell body and proximal dendrite in dioestrous and pro-oestrous female mice. An evaluation of all synapses immunoreactive for synaptophysin revealed that the highest density of inputs to rostral preoptic area GnRH neurons occurred within the first 45 μm of the primary dendrite (approximately 0.19 synapses μm^{-1}) with relatively few synapses on the GnRH neuron soma or beyond 45 μm of the dendrite (0.05-0.08 synapses μm^{-1}). Triple immunofluorescence labelling demonstrated a predominance of glutamatergic signalling with twice as many vesicular glutamate transporter 2 synapses detected compared to vesicular GABA transporter. Co-labelling with the $GABA_A$ receptor scaffold protein gephyrin and the glutamate receptor postsynaptic density marker Homer1 confirmed these observations, as well as the different spatial distribution of GABA and glutamate inputs along the dendrite. Quantitative assessments revealed no differences in synaptophysin, GABA or glutamate synapses at the proximal dendrite and soma of GnRH neurons between dioestrous and pro-oestrous mice. Taken together, these studies demonstrate that the GnRH neuron receives twice as many glutamatergic synapses compared to GABAergic synapses and that these inputs preferentially target the first 45 μm of the GnRH neuron proximal dendrite. These inputs appear to be structurally stable before the onset of pro-oestrous GnRH surge.

KEYWORDS

expansion microscopy, gephyrin, GnRH, homer, oestrous cycle, synaptophysin, VGAT, VGLUT2

1 | INTRODUCTION

The gonadotrophin-releasing hormone (GnRH) neurons represent the final output cells of the neural network controlling fertility in mammals. Driven by pulse and surge generators, GnRH neurons release GnRH into the median eminence in an episodic manner to create pulsatile or surge profiles of circulating gonadotrophin hormones.[1] The surge generator is only usually found in female mammals with the mid-cycle GnRH surge generating a luteinising hormone (LH) surge that triggers ovulation.[2]

Precisely how the GnRH neurons become suddenly and intensely activated to create the massive outpouring of GnRH that occurs at the surge remains unclear.[3,4] There is little doubt that sustained high levels of circulating oestradiol are obligatory for the GnRH surge in spontaneously ovulating mammals[5] and this is relayed to the GnRH neurons by afferent inputs that express the key oestrogen receptor, ESR1.[6-8] These neurons very likely target the GnRH neuron cell body and proximal dendrites to trigger the intense neuronal activation required for the surge.[9,10]

The prime candidate for triggering the surge is presently the ESR1-expressing kisspeptin neurons of the rostral periventricular area of the third ventricle (RP3V) that directly innervate the GnRH neuron cell body and dendrites.[11,12] However, there has been a long-standing interest and focus on the role of GABAergic and glutamatergic inputs to the GnRH neuron in surge generation.[3,4,13] For example, the deletion of ESR1 from all GABAergic or vesicular glutamate transporter 2 (VGLUT2)-glutamatergic neurons abolishes the LH surge likely independent of kisspeptin.[14] Electrophysiological studies have also reported that $GABA_A$ and glutamate receptor transmission at the GnRH neuron can change at the time of the LH surge,[15,16] although this depends on the animal model used.[17,18] Hence, it remains possible that steroid-induced plasticity in GABA and glutamate signalling to the GnRH neuron cell body may play a role in the generation of the GnRH/LH surge.

There is considerable evidence for gonadal steroids to evoke structural plasticity within the brain.[19] As such, the elevated follicular-phase levels of oestradiol may result in morphological rearrangements in GABAergic and glutamatergic inputs to the GnRH neuron cell body and proximal dendrites. Prior investigations have shown that GnRH neuron dendritic spine density increases at the time of the surge[20] although it remains unclear whether this involves GABA and glutamatergic inputs. Moore et al[21] recently examined this issue in an ovariectomised, oestradiol-treated mouse model and, surprisingly, found little change in the numbers of vesicular GABA transporter (VGAT) or VGLUT2-immunoreactive terminals opposing the GnRH neuron cell body and proximal dendrites around the time of the LH surge.

In the present study, we have taken advantage of recent developments in super-resolution microscopy to re-examine the issue of structural GABA and glutamate synaptic plasticity in relation to the GnRH neurons at the onset of the GnRH surge and done so in intact female mice. Expansion microscopy (ExM) utilises isotropic tissue swelling to expand the sample so that regular confocal imaging can achieve the necessary resolution required to identify bona fide synapses in the brain.[22]

2 | MATERIALS AND METHODS

2.1 | Mice

Female C57BL/6 GnRH-green fluorescent protein (GFP) mice[23] aged between 2 and 4 months old were used for immunohistochemistry and ExM. The mice were maintained under a 12:12-hour light/dark photocycle (lights off 6.00 PM) with access to food and water available ad lib. Experimental procedures were undertaken in accordance with the University of Otago Animal Welfare and Ethics Committee. Female GnRH-GFP mice exhibiting at least 3 regular oestrous cycles were killed for experiments between 2.00 PM and 4.00 PM on dioestrus (N = 4) or pro-oestrus (N = 4). The pro-oestrous LH surge commences at 5.00 PM (1 hour before lights off) in this mouse colony.[24]

2.2 | Immunohistochemistry

Mice received a fatal dose of pentobarbital (2 mg kg^{-1} body weight) and were perfused transcardially with 4% paraformaldehyde in 0.1 M phosphate-buffered saline (Sigma-Aldrich, St Louis, MO, USA; pH 7.6). Coronal brain sections of 50 μm thickness were cut using a vibratome and sections stored in cryoprotectant until used. Sections were pre-treated with 0.1% sodium borohydrate (Sigma-Aldrich) in Tris-buffered saline (TBS) for 15 min at room temperature and then further treated with 0.1% Triton-X-100 (Sigma-Aldrich) and 2% goat serum in TBS overnight at 4°C. Sections were then washed in TBS and incubated for 72 h at 4°C with different combinations of primary antisera added to the incubation solution containing TBS, 0.25% Triton-X-100, 0.3% bovine serum albumin and 2% goat serum. Antibodies for presynaptic markers were guinea pig anti-synaptophysin 1 (dilution 1:800; Synaptic Systems, Goettingen, Germany), rabbit anti-VGLUT2 (dilution 1:800; Synaptic Systems) and VGAT (dilution 1:800; Synaptic Systems). Guinea pig anti-gephyrin (dilution 1:800; Synaptic Systems) and guinea-pig anti-Homer1 (dilution 1:800; Synaptic Systems) were used for labelling postsynaptic markers. The specificity of the antibodies in mouse brain has been reported previously.[25-28] Controls were performed in the absence of one or both primary antibodies. Reabsorption of the Homer1 antisera was undertaken by incubation with Homer1 peptide for 48 h at 4°C. After washing, the sections were incubated with biotinylated anti-guinea pig immunoglobulins (IgG; Vector Laboratories, Burlingame, CA, USA) combined with Alexa 488-conjugated goat anti-chicken (Molecular Probes, Eugene, OR, USA) and ATTO 647-conjugated goat anti-rabbit (Sigma-Aldrich) secondary antibodies for 15 hours at 4°C. A full list of antisera used is provided in Table 1.

TABLE 1 List of antibodies and software

Reagent type	Designation	Source	Identifiers	Additional Information
Antibody	Anti-green fluorescent protein (chicken polyclonal)	Abcam (Cambridge, United Kingdom)	Abcam: AB13970 RRID:AB_300798	(1:8000)
Antibody	Anti-synaptophysin 1 (guinea pig polyclonal)	Synaptic Systems, Goettingen, Germany	Synaptic systems: 101 004 RRID:AB_1210382	(1:800)
Antibody	Anti-vesicular glutamate transporter 2 (rabbit polyclonal)	Synaptic Systems	Synaptic systems: 135 403 RRID:AB_887883	(1:800)
Antibody	Anti-vesicular GABA transporter (rabbit polyclonal)	Synaptic Systems	Synaptic systems: 131 003 RRID:AB_887869	(1:800)
Antibody	Anti-gephyrin (guinea pig polyclonal)	Synaptic Systems	Synaptic systems: 147 318 RRID:AB_2661777	(1:800)
Antibody	Anti-Homer I (guinea pig polyclonal)	Synaptic Systems	Synaptic systems: 160 004 RRID:AB_10549720	(1:800)
Antibody	Goat anti-chicken (goat polyclonal, Alexa488-conjugate)	Thermo Fisher Scientific, Waltham, MA, USA	Thermo Fisher Scientific: A-11039 RRID:AB_2534096	(1:200)
Antibody	Goat anti-guinea pig (goat polyclonal, biotin-conjugated)	Vector Laboratories, Burlingame, CA, USA	Vector Laboratories: BA-7000 RRID:AB_2336132	(1:200)
Antibody	Goat anti-rabbit (goat polyclonal, ATTO647N-conjugated)	Sigma-Aldrich, St Louis, MO, USA	Sigma-Aldrich: 40 839 RRID:AB_1137669	(1:200)
Software	ImageJ image analysis software	Version 2.0.0-rd-68 for MacOS (https://imagej.net/)	RRID:SCR_003070	
Software	GraphPad Prism	Version 8.3.1 for MacOS (www.graphpad.com)	RRID:SCR_002798	
Software	Vaa3D data visualisation software	Version 2.868 for MacOS (http://www.vaa3d.org)	RRID:SCR_002609	

2.3 | Expansion microscopy

The ExM was carried out as previously reported in detail.[10] After washing, sections were stained with 1:1000 Hoechst dye (Life Technologies, Carlsbad, CA, USA) for 15 min to label cell nuclei. Sections underwent linking with anchoring agent (methacrylic acid *N*-hydroxysuccinimide ester; 2 mM) for 1.5 hours and then incubation with monomer solution on ice for 45 minutes. Sections were then immersed in gelling solution within the gelation chamber at 37°C for 2 hours. The gelling solution is made from a combination of monomer solution, 0.01% 4-hydroxy TEMPO, 0.2% tetramethylethylenediamine and 0.2% ammonium persulfate in defined proportions. Next, the gel-embedded sections were trimmed and digested overnight with proteinase K at 37°C. The samples were incubated with strepavidin-568 (dilution 1:1500) at 37°C for 3 hours. The 568-fluorophore was not compatible with the gelation process; therefore, it was added after the gelation step. Increasing the incubation temperature improved the diffusion of streptavidin molecules in the gel. Finally, expansion was undertaken by adding water every 20 minutes, up to 5 times. Expanded samples were placed in an imaging chamber and cover slipped using #1.5 (0.17 mm) glass.

2.4 | Image analysis

The definition of a synapse with ExM relies on the detection of sufficient overlap between the fluorescent labels of the pre- and postsynaptic markers.[10] Although the tissue expansion increases the apparent final resolution of ExM into the superresolution realm, the confocal microscopy used for imaging the specimen is still diffraction-limited. This means that pre- and postsynaptic structures divided by a synaptic cleft even with this technique show some overlap of their image intensity profiles. Using VGAT and gephyrin immunofluorescence to define GABA synapses on GnRH-GFP neurons, we have previously calculated that, with our microscope (see details below), the overlap between a presynaptic marker and cytoplasmic GFP in a GnRH-GFP neuron must be > 0.95 μm (0.23 μm pre-expansion) in the "side-on" fluorescence profile view to be considered a synapse[10] (ie, every VGAT-gephyrin synapse has an overlap between VGAT and GnRH-GFP fluorescence greater than 0.95 μm). Not all synapses can be rotated to provide a side-on view and, in those cases, a "z-stack/face-view" profile of multiple imaged synapses is required and with this orientation, the fluorescence needs to overlap by > 1.75 μm (0.42 μm pre-expansion) to account for decreased resolution along this imaging axis and to be considered a synapse.[10] To determine the degree of tissue swelling, the diameter of the nuclei of individual GnRH neurons were measured before and after gelation.

All imaging was performed using an A1R upright confocal microscope (Nikon, Tokyo, Japan) with images captured using a water-immersion lens (25× NA 1.1; working distance 2 mm). Alexa Fluor 488, Alexa Fluor 568 (BD Biosciences, Frankin Lakes, NJ, USA) and ATTO 647 (ATTO-TEC, Siegen, Germany) were excited with 488, 561 and 640 nm laser lines and emission was collected in the ranges 500-550 nm, 580-620 nm and 620-660 nm bandpass emission filters, respectively. All images were captured using sequential scanning mode and image stacks (frames: 102.51 × 51.25 μm, 1024 × 512 pixels) were collected with focus intervals of 0.6 μm. Images were analysed using ImageJ (NIH, Bethesda, MD, USA) and GnRH neurons were selected at random from three rostral preoptic area sections in each mouse. In total, 250 μm (60 μm pre-expansion) of continuous primary dendrite extending from the GnRH cell body was imaged sequentially. Synaptophysin/VGLUT2/VGAT boutons that were more than 0.4 μm in diameter and in apparent close contact with a GnRH-GFP soma or proximal dendrite were selected for the line scan or z-stack analysis. A line scan was performed and the relative intensity of the Alexa Fluor 488 and Alexa Fluor 568 or ATTTO 647 was measured and plotted in Excel (Microsoft Corp., Redmond, WA, USA). For the z-stack face view orientation, a 2 μm × 2 μm (width × length) box was drawn over the bouton to measure the average intensity of each channel in z-stack through the scan. Appositions meeting the criteria noted above were counted as synapses. The distribution of synaptophysin, glutamatergic and GABAergic synapses were mapped to the entire soma and four 15 μm-lengths of the proximal dendrite: 0-15 μm, 16-30 μm, 31-45 μm and 46-60 μm to maintain consistency with previous studies.[20,21] Three-dimensional reconstructions of GnRH proximal dendrites displaying synaptophysin appositions were performed with an Open Source visualisation and analysis software suite, Vaa3D.[29]

2.5 | Statistical analysis

Statistical analyses were performed using Prism (GraphPad Software Inc., San Diego, CA, USA). Two-way ANOVA with repeated-measures was applied to compare the mean number of synapses on soma and on dendrite segments every 15 μm between pro-oestrous and dioestrous animals. Full statistical details for each analysis are provided in Table 2.

3 | RESULTS

By assessing the size of the GnRH neuron nuclei before and after expansion, we determined that the ExM procedure enlarged brain sections by a factor of 4.17 ± 0.01 (n = 43).

3.1 | Distribution of synaptic inputs along the GnRH neuron soma and proximal dendrite

We first assessed the distribution of all synapses along the GnRH neuron using synaptophysin as a general presynaptic marker.[21,30] All mice exhibited GnRH neurons surrounded by typical punctate synaptophysin immunoreactivity (Figure 1) that was completely absent when the primary antibody was omitted from the immunohistochemistry (not shown). Many close appositions were detected

TABLE 2 Statistical reporting

Figure 2C					
Two-way repeated measures ANOVA					
Assume sphericity?	Yes				
Alpha	0.05				
ANOVA	SS	*df*	MS	$F\ (df_n, df_d)$	*P* value
Synapse × Oestrous Cycle	10.40	4	2.6	$F_{4,24} = 1.396$	$P = 0.2653$
Synapse	1353.00	4	338.2	$F_{4,24} = 181.6$	$P < 0.0001$
Oestrous cycle	0.23	1	0.225	$F_{1,6} = 0.2061$	$P = 0.6658$
Subject	6.55	6	1.092	$F_{6,24} = 0.5861$	$P = 0.7380$
Residual	44.70	24	1.863		
Figure 3B					
Two-way repeated measures ANOVA					
Assume sphericity?	Yes				
Alpha	0.05				
ANOVA	SS	*df*	MS	$F\ (df_n, df_d)$	*P* value
Synapse × Oestrous Cycle	4.85	4	1.213	$F_{4,24} = 1.500$	$P = 0.2336$
Synapse	135.40	4	33.84	$F_{4,24} = 41.86$	$P < 0.0001$
Oestrous cycle	0.40	1	0.4	$F_{1,6} = 0.6667$	$P = 0.4454$
Subject	3.60	6	0.6	$F_{6,24} = 0.7423$	$P = 0.6211$
Residual	19.40	24	0.8083		
Figure 3D					
Two-way repeated measures ANOVA					
Assume sphericity?	Yes				
Alpha	0.05				
ANOVA	SS	*df*	MS	$F\ (df_n, df_d)$	*P* value
Synapse × Oestrous Cycle	1.60	4	0.4	$F_{4,24} = 0.5647$	$P = 0.6906$
Synapse	51.40	4	12.85	$F_{4,24} = 18.14$	$P < 0.0001$
Oestrous Cycle	0.40	1	0.4	$F_{1,6} = 1.200$	$P = 0.3153$
Subject	2.00	6	0.3333	$F_{4,24} = 0.4706$	$P = 0.8232$
Residual	17.00	24	0.7083		
Figure 5C					
Two-way repeated measures ANOVA					
Assume sphericity?	Yes				

(Continues)

TABLE 2 (Continued)

Figure 2C					
Alpha	0.05				
ANOVA	SS	*df*	MS	$F\ (df_n, df_d)$	*P* value
Synapse × Oestrous Cycle	0.67	4	0.1667	$F_{4,16} = 0.1010$	$P = 0.9805$
Synapse	80.53	4	20.13	$F_{4,16} = 12.20$	$P = 0.0035$
Oestrous Cycle	0.83	1	0.8333	$F_{1,4} = 0.1645$	$P = 0.7058$
Subject	20.27	4	5.067	$F_{4,16} = 3.071$	$P = 0.0469$
Residual	26.40	16	1.65		
Figure 6C					
Two-way repeated measures ANOVA					
Assume sphericity?	Yes				
Alpha	0.05				
ANOVA	SS	*df*	MS	$F\ (df_n, df_d)$	*P* value
Synapse × Oestrous Cycle	0.33	4	0.08333	$F_{4,16} = 0.1042$	$P = 0.9794$
Synapse	8.87	4	2.217	$F_{4,16} = 2.771$	$P = 0.0634$
Oestrous Cycle	0.83	1	0.8333	$F_{1,4} = 1.786$	$P = 0.2524$
Subject	1.87	4	0.4667	$F_{4,16} = 0.5833$	$P = 0.6792$
Residual	12.80	16	0.8		

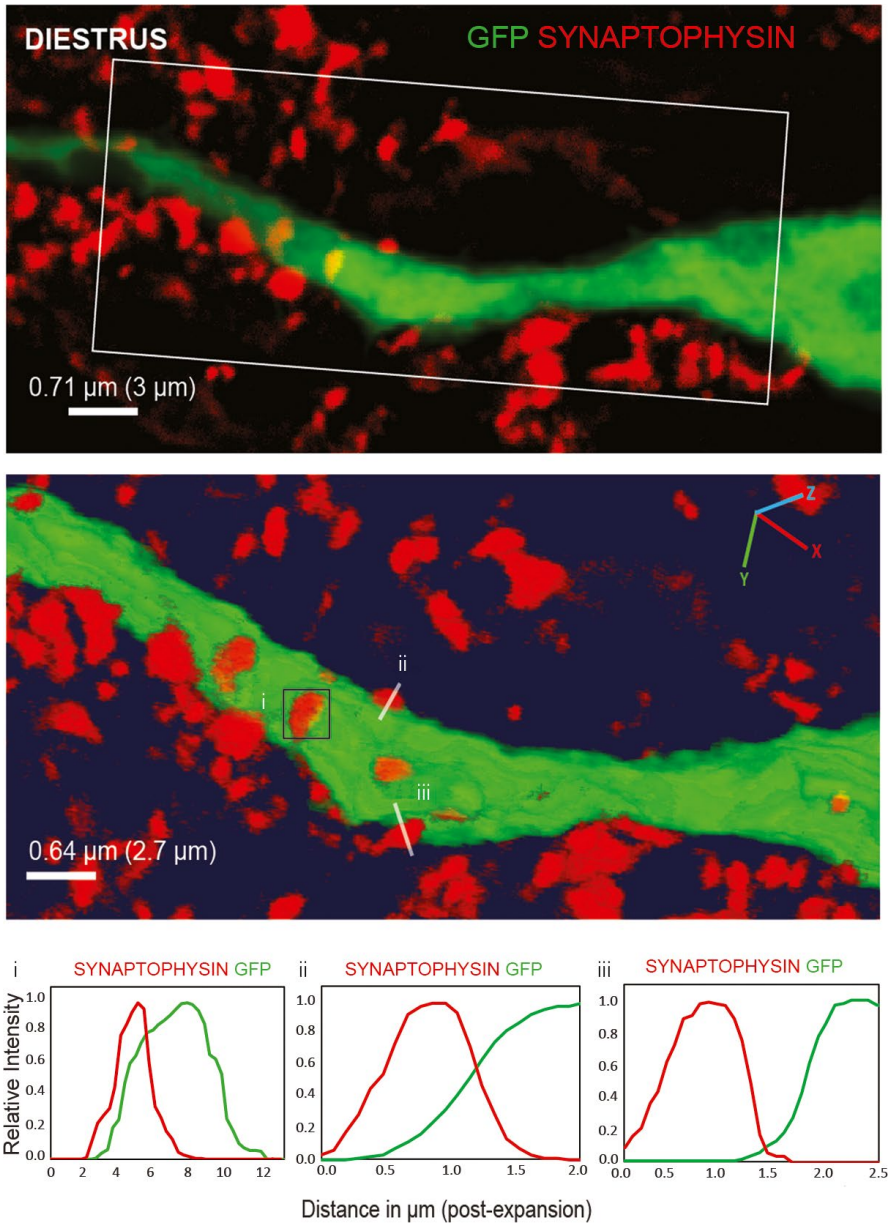

FIGURE 1 Expansion microscopy image showing multiple synaptophysin boutons (Alexa Fluor 568, red) surrounding the proximal dendrite of a green fluorescent protein (GFP)-expressing gonadotrophin-releasing hormone (GnRH) neuron (Alexa Fluor 488, green) in a female GnRH-GFP mouse. A three-dimensional reconstruction of the dendrite is provided below in which three appositions (i-iii) are analysed using linear or square regions of interest (ROIs) (bottom) to determine the proximity of each synaptophysin bouton to the dendrite. Apposition (i) is analysed in the face-view (z-axis, square ROI), whereas (ii) and (iii) are analysed in the side-on view (linear ROI). Appositions (i) and (ii) represent synapses with an overlap in synaptophysin fluorescence and GnRH-GFP fluorescence that is > 1.75 µm (0.42 µm pre-expansion) in the face-view (i) and > 0.95 µm (0.23 µm pre-expansion) in the side-on view (ii). Apposition iii does not represent a synapse. Scale bars give pre-expansion values with the post-expansion scale in brackets

between synaptophysin boutons and GnRH neurons but only some satisfied the criteria for a synapse. Figure 1 shows examples of bona fide synapses in the z-stack face-on view (Figure 1i) and side-on view (Figure 1ii) and a close apposition that is not forming a direct synapse (Figure 1iii). Quantitative analysis revealed that the average density of synapses peaked in the 0-45 µm segment of the proximal dendrite (0.19 ± 0.01 synapses μm^{-1}) compared to the soma (0.08 ± 0.01 synapses μm^{-1}) and beyond 45 µm on the dendrite (0.05 ± 0.01 synapses μm^{-1}) (Figure 2 and Table 3). No significant differences in the numbers of synaptophysin-defined synapses were detected between dioestrous (24 neurons, N = 4) and pro-oestrous mice (24 neurons, N = 4) (two-way repeated-measures ANOVA, $P = 0.27$) (Figure 2C). The average synaptic densities across the soma and first 60 µm of proximal dendrite were 0.17 ± 0.01 synapses μm^{-1} at dioestrous and 0.16 ± 0.01 synapses μm^{-1} at pro-oestrous.

3.2 | Distribution of GABAergic and glutamatergic inputs along the GnRH neuron soma and proximal dendrite

We assessed glutamatergic and GABAergic inputs to the GnRH neuron by labelling for synaptophysin and GFP combined with the presynaptic markers VGAT or VGLUT2. The specificity of VGAT and VGLUT2 antibodies have been described previously.[25,26] The absence of primary antibodies in the present experiments resulted in no detectable immunofluorescence (not shown).

Glutamatergic synapses were defined as being boutons that contained both synaptophysin and VGLUT2 immunofluorescence that formed a sufficient ExM overlap with the cytoplasmic GFP of the GnRH neuron (Figure 3A). Spatial analysis revealed a distribution of VGLUT2 synaptic density that was similar to that of synaptophysin with relatively high densities in the 0-45-µm segment of the

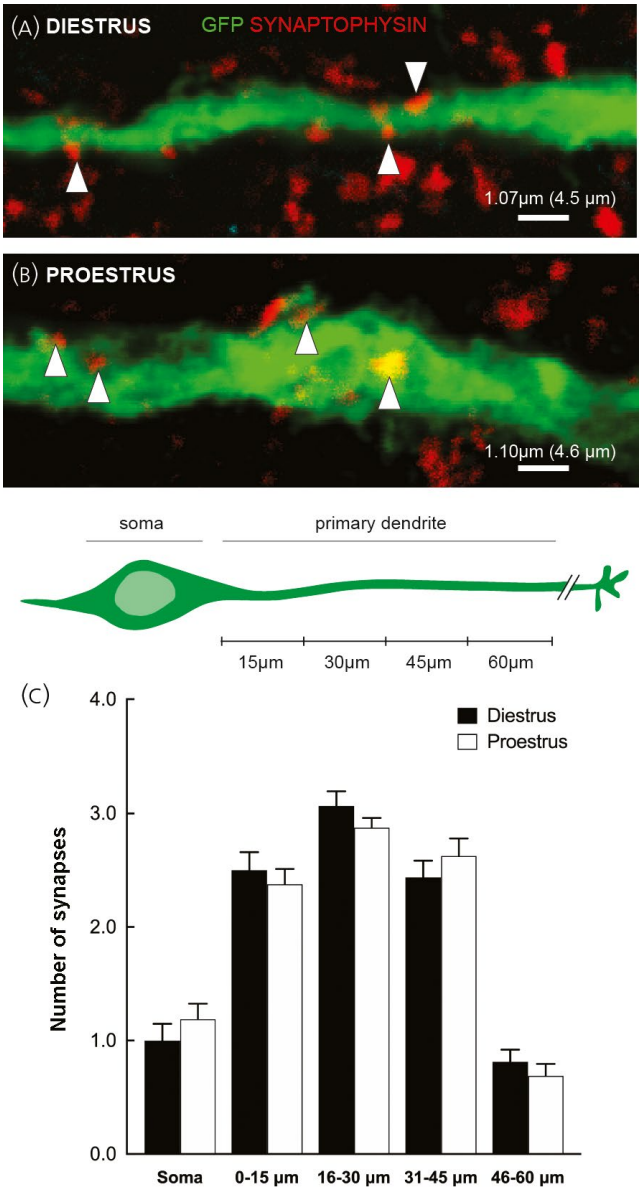

FIGURE 2 Distribution of synaptophysin synapses on gonadotrophin-releasing hormone (GnRH) neuron cell bodies and proximal dendrites. A and B, Expansion microscopy images showing multiple synaptophysin boutons apposing green fluorescent protein (GFP)-filled GnRH proximal dendrites within a 9-μm segment (pre-expansion) in dioestrous (A) and pro-oestrous (B) mice. C, Histogram showing the mean ± SEM number of synaptophysin synapses identified on the GnRH neuron soma and sequential 15-μm segments of the proximal dendrite in dioestrous (black bars, 24 neurons from 4 mice) and pro-oestrous (open bars, 24 neurons from 4 mice) mice killed just prior to the onset of the luteinising hormone (LH) surge. No significant differences were detected. Scale bars give pre-expansion values with the post-expansion scale in brackets

proximal dendrite (approximately 0.09 synapses μm^{-1}) (Figure 3B) compared to the soma or more distal on the dendrite (approximately 0.03 synapses μm^{-1}) (Table 3). No significant differences were detected between dioestrous (16 neurons, N = 4) and pro-oestrous mice (16 neurons, N = 4) (two-way repeated-measures ANOVA, $P = 0.23$). Overall synaptic densities for the proximal dendrite (0-60 μm) were 0.08 ± 0.01 μm^{-1} in dioestrus and 0.07 ± 0.01 μm^{-1} in pro-oestrus and 0.03 ± 0.01 μm^{-1} for the soma in both stages of the cycle (Figure 3B). The densities per 15-μm segment are given in Table 3.

GABAergic synapses were similarly defined as locations where boutons containing both synaptophysin and VGAT formed a sufficient overlap with cytoplasmic GFP (Figure 3C). In this case, we found that GABAergic synapses were clustered predominantly in the 16-45-μm segment of the proximal dendrite (approximately 0.06 synapses μm^{-1}) with very few synapses detected elsewhere (Figure 3D and Table 3). Again, no differences were detected between dioestrous (16 cells, N = 4) and pro-oestrous mice (16 cells, N = 4) with overall dendritic (0-60 μm) synaptic densities being 0.04 ± 0.01 μm^{-1} and 0.03 ± 0.01 μm^{-1}, respectively, and 0.01 ± 0.01 μm on the soma for both dioestrus and pro-oestrus (two-way repeated-measures ANOVA, $P = 0.69$) (Figure 3B). The densities per 15-μm segment are given in Table 3.

An alternative and potentially more definitive method for determining glutamatergic and GABAergic synapses is to combine the presynaptic markers VGLUT2 and VGAT with postsynaptic markers for glutamatergic and GABAergic synapses. Practically, choices for the latter are restricted to proteins that have antisera well characterised to work in mouse brain tissue. We used Homer1, a scaffold protein at glutamatergic synapses[31] and gephyrin that clusters $GABA_A$ receptors to synapses.[32] Synapses were defined as locations where Homer1/gephyrin immunoreactivity within the GFP-tagged cytoplasm overlapped with the presynaptic VGLUT2/VGAT immunofluorescence as defined above (Figure 4). The specificity of the gephyrin antibody has been validated previously.[27]Homer1 antisera preadsorbed with Homer1 control peptide eliminated all labelling.

For glutamate, VGLUT2-Homer1 synapses were detected with increasing density along the primary dendrite to peak at the 31-45-μm segment with an abrupt decline thereafter (Figure 5). The average density of this segment in dioestrous mice is 0.08 ± 0.02 synapses μm^{-1} and 0.07 ± 0.02 synapses μm^{-1} in pro-oestrous mice. Very few VGLUT2-Homer1 synapses were detected on the soma (Figure 5C). No differences were detected between dioestrous (13 cells, N = 4) and pro-oestrous mice (12 cells, N = 4) (two-way repeated-measures ANOVA, $P = 0.98$). Average synaptic densities along the 0-60 μm of the dendrite were 0.03 ± 0.01 μm^{-1} in dioestrous and pro-oestrous mice (Figure 5C). Densities per 15-μm segment are given in Table 3.

For GABA inputs, a low density of VGAT-gephyrin synapses was detected along the dendrite with very few (0-0.01 synapses μm^{-1}) on the soma (Figure 6 and Table 3). Peak density on the primary dendrite was observed in the 16-45-μm segment, at 0.03 ± 0.07 synapses μm^{-1}. No significant differences were detected between GnRH neurons from dioestrous (10 cells, N = 4) and pro-oestrous mice (12 cells, N = 4) (two-way repeated-measures ANOVA, $P = 0.98$) (Figure 6C).

TABLE 3 Densities of synaptic inputs on the gonadotrophin-releasing hormone neuron soma and sequential 15 micrometer segments of their proximal dendrites (density of synapses/μm, mean ± SEM)

Synaptophysin	Dioestrus (n = 24 cells)	Pro-oestrus (n = 24 cells)
Soma	0.08 ± 0.01	0.09 ± 0.01
0-15 μm	0.17 ± 0.01	0.16 ± 0.01
16-30 μm	0.20 ± 0.01	0.19 ± 0.01
31-45 μm	0.16 ± 0.01	0.18 ± 0.01
46-60 μm	0.05 ± 0.01	0.05 ± 0.01
VGLUT2-synaptophysin	**Dioestrus (n = 16 cells)**	**Pro-oestrus (n = 16 cells)**
Soma	0.03 ± 0.01	0.03 ± 0.01
0-15 μm	0.07 ± 0.01	0.06 ± 0.01
16-30 μm	0.10 ± 0.01	0.08 ± 0.01
31-45 μm	0.11 ± 0.01	0.10 ± 0.01
46-60 μm	0.02 ± 0.01	0.04 ± 0.01
VGAT-synaptophysin	**Dioestrus (n = 16 cells)**	**Pro-oestrus (n = 16 cells)**
Soma	0.01 ± 0.01	0.01 ± 0.01
0-15 μm	0.02 ± 0.01	0.01 ± 0.01
16-30 μm	0.05 ± 0.01	0.04 ± 0.01
31-45 μm	0.06 ± 0.01	0.05 ± 0.01
46-60 μm	0.01 ± 0.01	0.02 ± 0.01
VGLUT2-Homer1	**Dioestrus (n = 13 cells)**	**Pro-oestrus (n = 12 cells)**
Soma	0.01 ± 0.01	0.01 ± 0.01
0-15 μm	0.02 ± 0.01	0.02 ± 0.01
16-30 μm	0.06 ± 0.01	0.05 ± 0.02
31-45 μm	0.08 ± 0.02	0.07 ± 0.02
46-60 μm	0.02 ± 0.01	0.01 ± 0.01
VGAT-gephyrin	**Dioestrus (n = 10 cells)**	**Pro-oestrus (n = 12 cells)**
Soma	0	0.01 ± 0.01
0-15 μm	0.01 ± 0.01	0.01 ± 0.01
16-30 μm	0.02 ± 0.01	0.02 ± 0.01
31-45 μm	0.03 ± 0.02	0.03 ± 0.01
46-60 μm	0.01 ± 0.01	0.01 ± 0.01

Abbreviations: VGAT, vesicular GABA transporter; VGLUT2, vesicular glutamate transporter 2.

4 | DISCUSSION

In the present study, we report the density and spatial distribution of synaptic inputs to the mouse GnRH neuron cell body and proximal dendrite using ExM. This methodology has gained rapid popularity in neuroscience because of its ability to overcome the inadequate resolution afforded by conventional confocal microscopy to define a synapse.[22] Serial ultrastructural reconstructions have demonstrated that only approximately 10% of axons apposed to a dendritic spine actually form a synapse, raising caution when interpreting confocal apposition data.[33] Accordingly, we note that the densities of synaptophysin, VGAT and VGLUT2 synapses reported here on GnRH neurons are 4- to 5-fold lower than the numbers of appositions detected with regular confocal analysis in a similar mouse model.[21] Nevertheless, ExM remains dependent upon immunohistochemical detection and the degree to which synapses are under-represented with this approach is unclear. The density of spines on mouse GnRH neurons,[20,34] which would reasonably be assumed to represent sites of synaptic input, is approximately double that reported here for synaptophysin-defined synapses with ExM.

One of the most striking observations in the present study was that synaptic inputs to the GnRH neuron were differentially clustered into the first 45 μm of proximal dendrite with many fewer inputs to the cell body or beyond 45 μm. The low density of synaptic inputs to the cell body is reminiscent of early electron microscopic analyses that found very few, if any, synapses on the cell body of GnRH neurons.[35] The more extensive analysis of the GnRH neuron dendrites afforded by dye-filling GnRH neurons in situ has

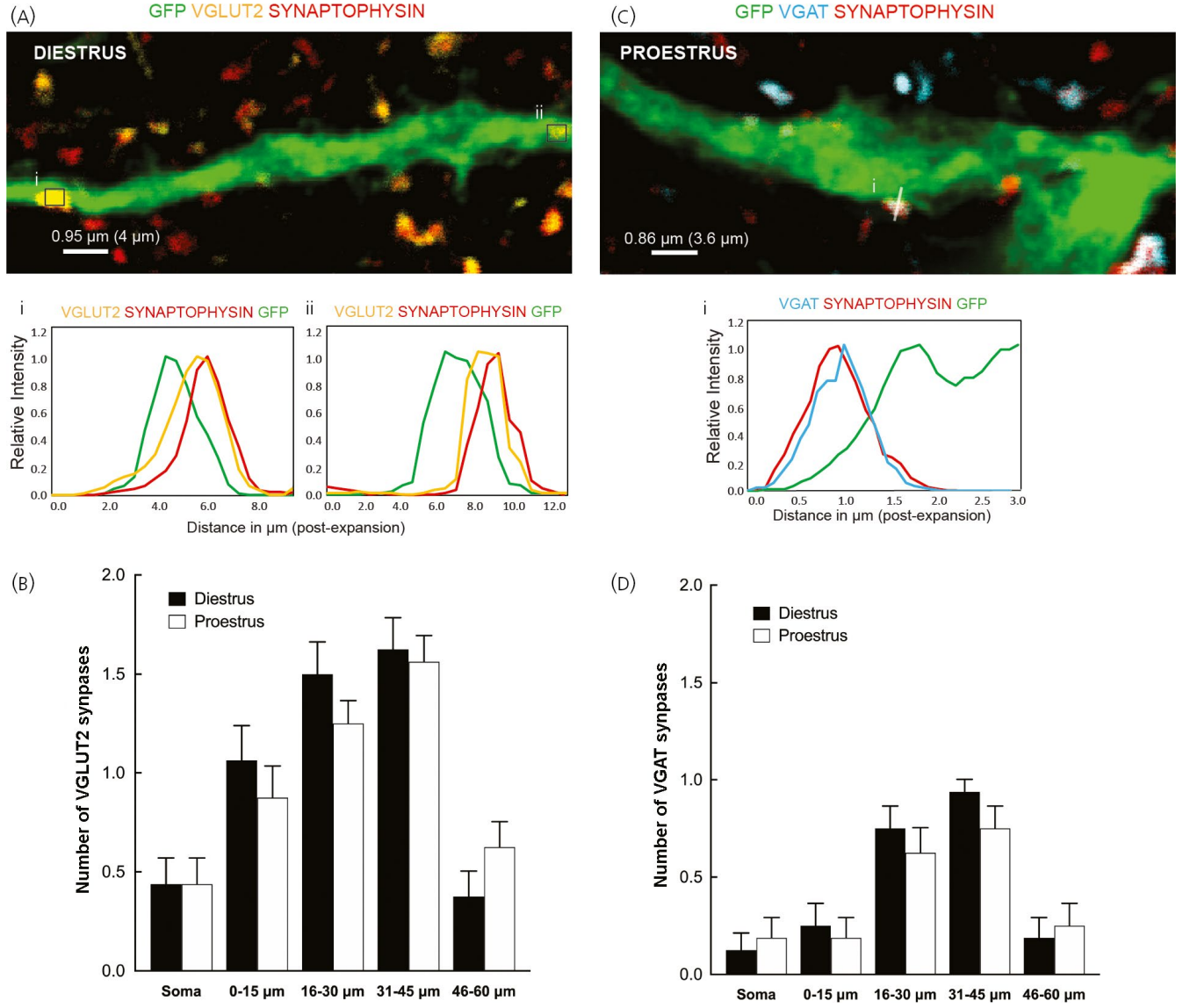

FIGURE 3 Distribution of GABA and glutamate synapses on gonadotrophin-releasing hormone (GnRH) neuron cell bodies and proximal dendrites. A, Expansion microscopy image showing vesicular glutamate transporter 2 (VGLUT2)-colocalised synaptophysin boutons apposing a green fluorescent protein (GFP)-expressing GnRH neuron proximal dendrite in a dioestrous female GnRH-GFP mouse. These boutons (i-ii) are analysed using square regions of interest (ROIs) in the face-view (z-axis) showing an overlap of > 1.75 µm (0.42 µm pre-expansion) between VGLUT2-colocalised synaptophysin fluorescence (VGLUT2 - ATTO 647, yellow; synaptophysin - Alexa Fluor 568, red) and GnRH-GFP fluorescence (Alexa Fluor 488, green). B, Histogram displaying the mean ± SEM number of VGLUT2-colabelled synaptophysin boutons found on GnRH soma and consecutive 15-µm segments of the proximal dendrite in dioestrous (black bars, 16 neurons from 4 mice) and pro-oestrous mice (open bars, 16 neurons from 4 mice). No significant differences were found. C, Expansion microscopy image demonstrating a vesicular GABA transporter (VGAT)-colocalised synaptophysin bouton on a GFP-filled GnRH proximal dendrite of a pro-oestrous GnRH-GFP mouse. (i) (below), Line ROI analysis of the VGAT-colabelled synaptophysin bouton displaying an overlap of at least 0.95 µm (side-view plane) between VGAT+synaptophysin fluorescence (VGAT - ATTO 647, cyan; synaptophysin - Alexa Fluor 568, red) and GnRH-GFP fluorescence (Alexa Fluor 488; green). D, Histogram showing the mean ± SEM number of VGAT-colocalised synaptophysin boutons found on GnRH soma and sequential 15-µm segments of the proximal dendrite. There were no significant differences between dioestrous (black bars, 16 neurons from 4 mice) and pro-oestrous mice (open bars, 16 neurons from 4 mice). Scale bars indicate pre-expansion values with the post-expansion scale in brackets

similarly shown that the highest density of spines occurs with the first 50 µm of dendrite with values halving beyond this.[34] We have recently reported that the highest density of synaptic inputs to the GnRH neuron occurs at its distal-most projections, the dendrons, just before they pass into the median eminence.[10] This indicates that GnRH neurons have two sites of high density synaptic input; one in the proximal dendrite near the cell body and the other at the distal dendrons.

We find here that GABA and glutamate inputs within this dendritic "hot spot" have distinct spatial distributions. As reflected in both the

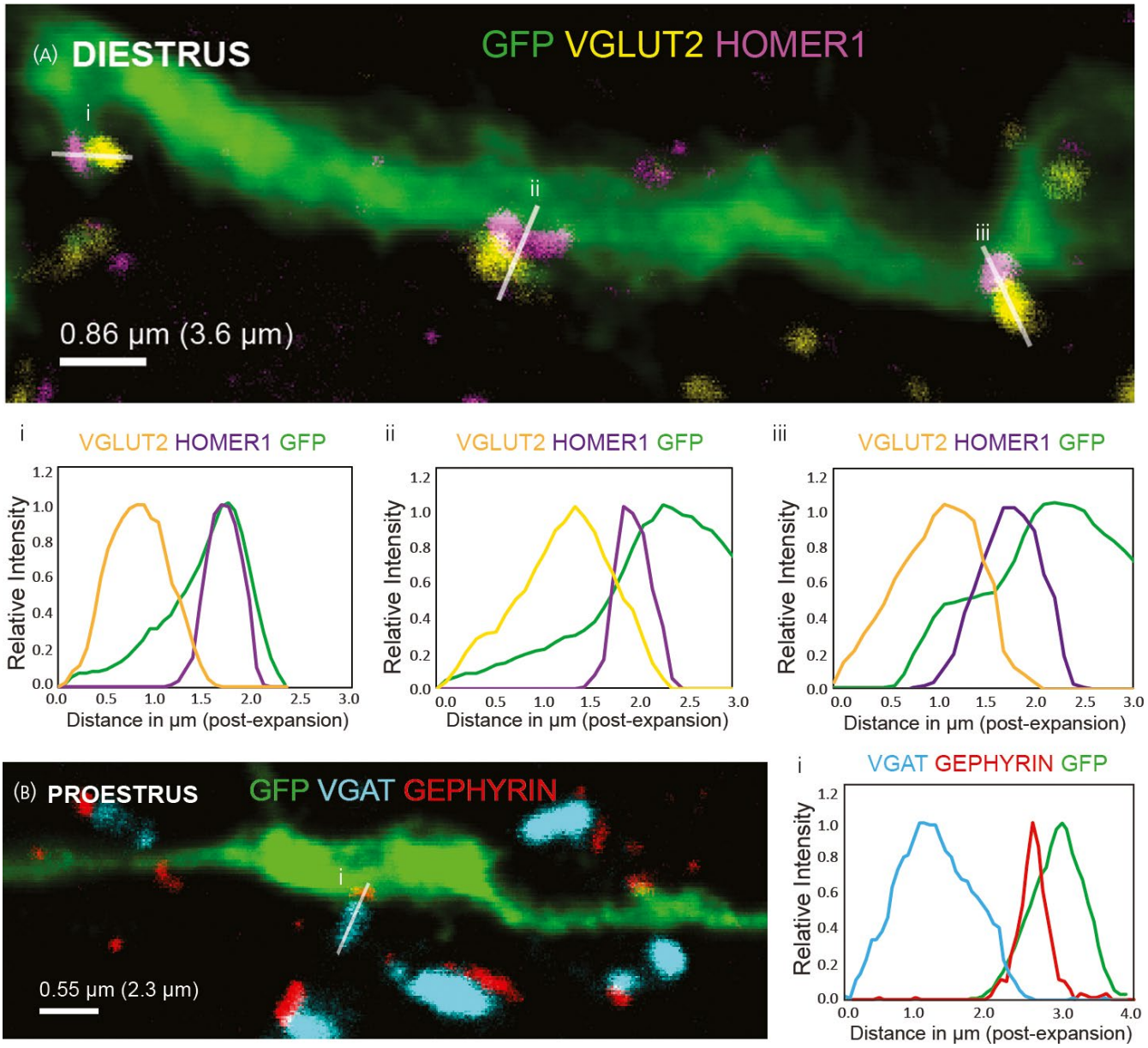

FIGURE 4 Glutamate-Homer and $GABA_A$ receptor synapses on gonadotrophin-releasing hormone (GnRH) neuron cell bodies and proximal dendrites. A, Expansion microscopy image showing vesicular glutamate transporter 2 (VGLUT2)-Homer1 synapses on a green fluorescent protein (GFP)-expressing GnRH neuron proximal dendrite in a dioestrous female GnRH-GFP mouse. (i-iii), Individual VGLUT2-Homer1 synapses analysed in the side-on view using line regions of interest (ROIs), demonstrating an overlap of at least 0.95 µm between VGLUT2 fluorescence (ATTO 647, yellow) and GnRH-GFP fluorescence (Alexa Fluor 488, green), with the presence of postsynaptic Homer1 (Alexa Fluor 568, magenta) within the GnRH neuron proximal dendrite. B, Expansion microscopy image showing a $GABA_A$ (vesicular GABA transporter [VGAT]-gephyrin) synapse on the proximal dendrite of a dioestrous GnRH-GFP neuron. (i), Line ROI analysis of the VGAT-gephyrin synapse displaying an overlap of at least 0.95 µm (side-view plane) between the VGAT fluorescence (ATTO 647; cyan) and GnRH-GFP fluorescence (Alexa Fluor 488; green) and the presence of postsynaptic gephyrin (Alexa Fluor 568, red) within the GnRH proximal dendrite. Scale bars show pre-expansion values with the post-expansion scale in brackets

VGLUT2-synaptophysin and VGLUT2-homer analyses, the density of glutamatergic inputs increased gradually along the dendrite until dropping precipitously after 45 µm. By contrast, GABAergic inputs, again seen in both VGAT-synaptophysin and VGAT-gephyrin experiments, were evenly concentrated in just the 16 - 45-µm segment of the dendrite. These data demonstrate that this 30-µm compartment of the dendrite receives abundant glutamatergic and GABAergic excitatory drive, suggesting that it may be involved in action potential initiation for the surge. Interestingly, analysis with electrophysiology and ankyrin-G immunohistochemistry demonstrates that the approximately 30-µm long action potential initiation site of GnRH neurons is typically located around 100 µm out on one of the dendrites.[36,37] It was not possible to include an ankyrin-G label in the present studies, but the present observations suggest that the

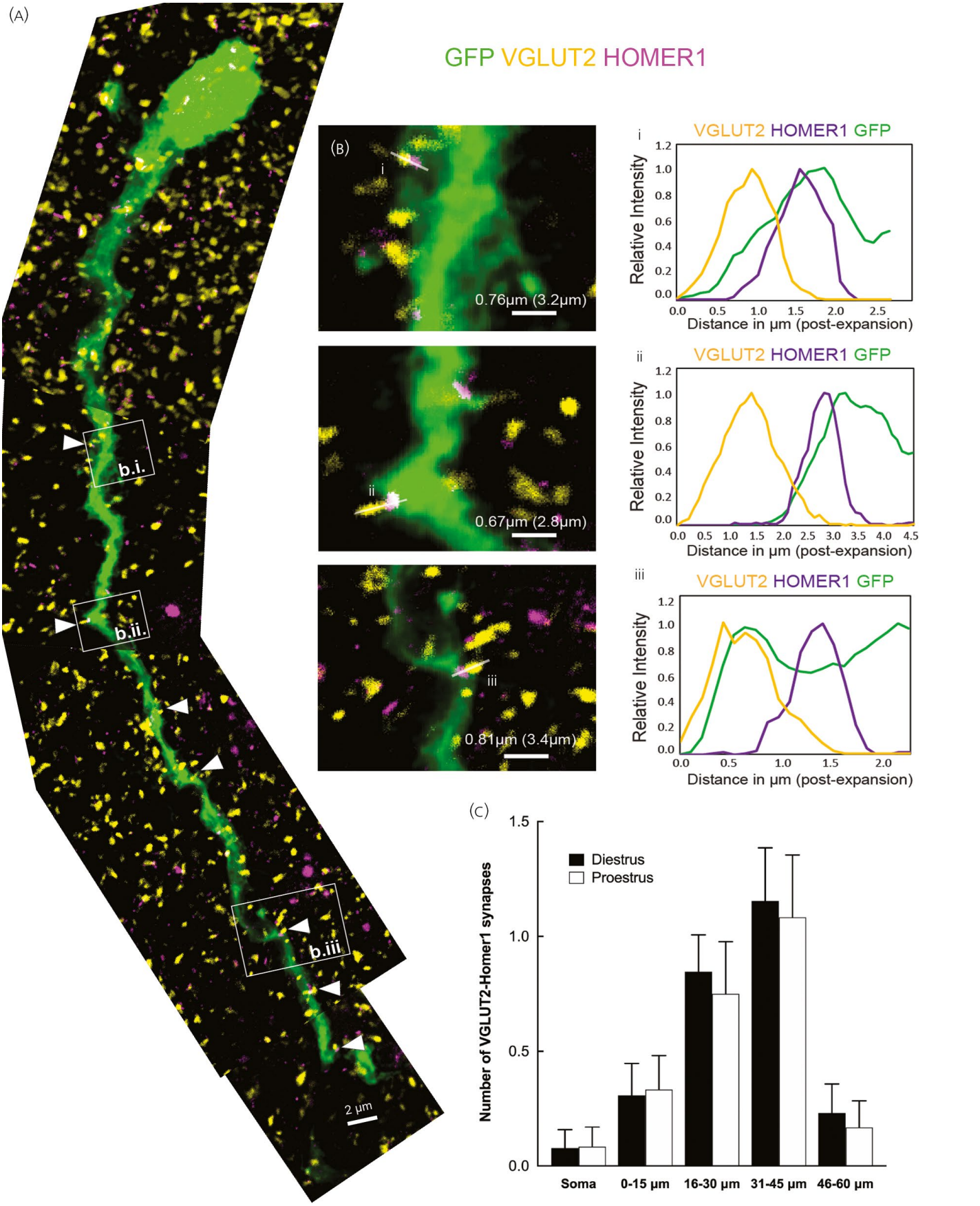
(A)
GFP VGLUT2 HOMER1
b.i.
b.ii.
b.iii.
2 µm
(B)
i
0.76µm (3.2µm)
ii
0.67µm (2.8µm)
iii
0.81µm (3.4µm)
i
VGLUT2 HOMER1 GFP
Relative Intensity
Distance in µm (post-expansion)
ii
VGLUT2 HOMER1 GFP
Relative Intensity
Distance in µm (post-expansion)
iii
VGLUT2 HOMER1 GFP
Relative Intensity
Distance in µm (post-expansion)
(C)
Diestrus
Proestrus
Number of VGLUT2-Homer1 synapses
Soma
0-15 µm
16-30 µm
31-45 µm
46-60 µm

FIGURE 5 Distribution of vesicular glutamate transporter 2 (VGLUT2)-Homer1 synapses on gonadotrophin-releasing hormone (GnRH) neuron cell bodies and proximal dendrites. A, Expansion microscopy images stitched together to delineate the spatial distribution of VGLUT2-Homer1 synapses (indicated by white triangles) on GnRH neural soma and proximal dendrite in a dioestrous female GnRH-green fluorescent protein (GFP) mouse. B (i-iii), Higher magnification images of the selected regions showing side-views of VGLUT2-Homer1 synapses on the GFP-filled GnRH neuron proximal dendrite with an overlap of > 0.95 μm (0.23 μm pre-expansion) in VGLUT2 fluorescence (ATTO 647, yellow) and GnRH-GFP fluorescence (Alexa Fluor 488, green). C, Histogram showing the mean ± SEM number of VGLUT2-Homer1 synapses found on the GnRH neuron soma and consecutive 15-μm segments of the proximal dendrite in dioestrous (black bars, 13 neurons from 4 mice) and pro-oestrous mice (open bars, 12 neurons from 4 mice). No significant differences were observed. Scale bars indicate pre-expansion values with the post-expansion scale in brackets

FIGURE 6 Distribution of vesicular GABA transporter (VGAT)-gephyrin synapses on gonadotrophin-releasing hormone (GnRH) neuron cell bodies and proximal dendrites. A, Expansion microscopy images demonstrating the relatively sparse distribution of VGAT-gephyrin synapses (indicated with white triangles) on the GnRH neuron proximal dendrite of a pro-oestrous female GnRH-green fluorescent protein (GFP) mouse. B, Higher magnification image of a region displaying VGAT-gephyrin synapses on a GFP-tagged GnRH proximal dendrite in side-view (i) with an overlap of > 0.95 μm (0.23 μm pre-expansion) and in face-view (ii) with an overlap of > 1.75 μm (0.42 μm pre-expansion) in VGAT fluorescence (ATTO 647, cyan) and GnRH-GFP fluorescence (Alexa Fluor 488, green). C, Histogram showing the mean ± SEM number of VGAT-gephyrin synapses found on the GnRH neuron soma and sequential 15-μm segments of the proximal dendrite. No significant differences were identified in dioestrous (black bars, 10 neurons from 4 mice) and pro-oestrous mice (open bars, 12 neurons from 4 mice). Scale bars show pre-expansion values with the post-expansion scale in brackets

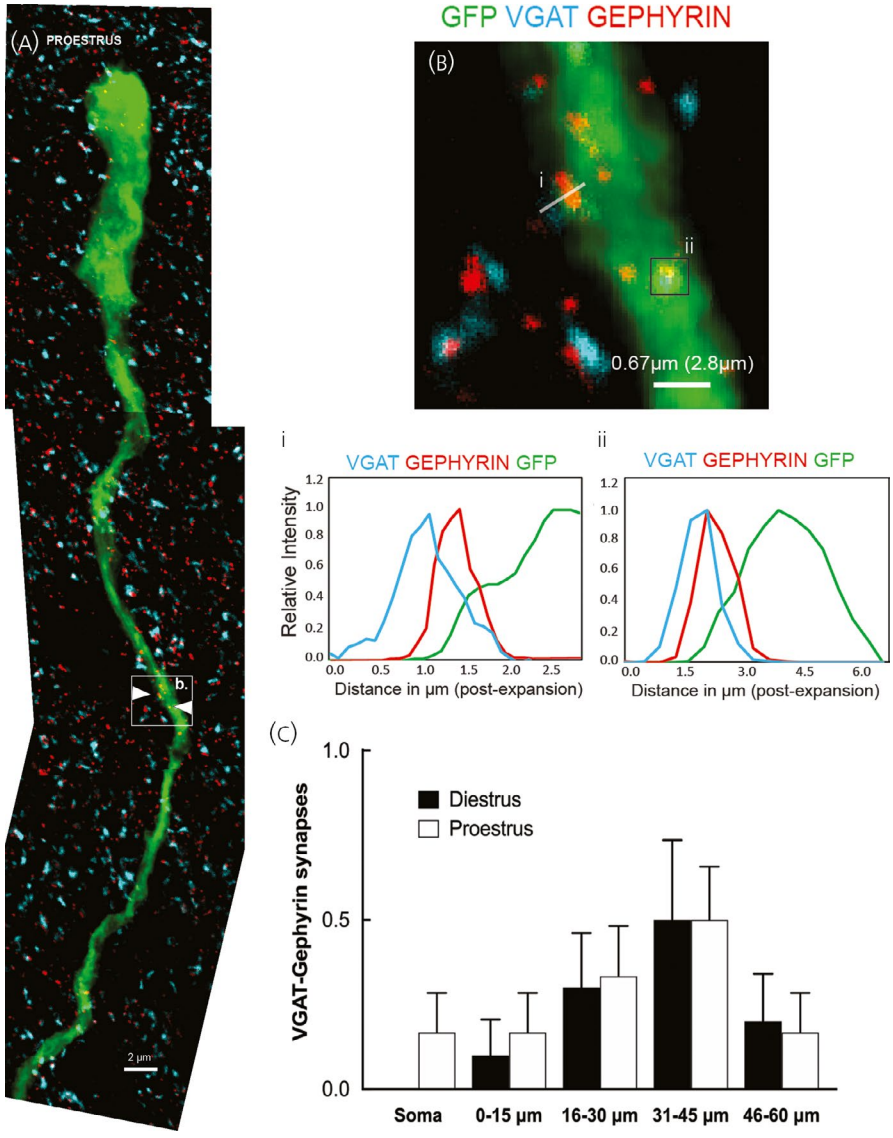

excitatory "hot-spot" on the dendrite is proximal to, rather than at, the action potential initiation site.

Although we cannot necessarily assume equal efficiencies of our vGLUT2 and VGAT immunohistochemistry, it appears that there are twice as many glutamatergic as GABAergic inputs to the GnRH neuron cell soma and proximal dendrite. This has not been detected previously. Although the frequency of $GABA_A$ receptor-mediated postsynaptic currents recorded from the GnRH neuron cell body is typically much higher than that of AMPA receptor-mediated events,[4,38] it is important to consider that these events reflect spontaneous release rates as much as the numbers of synapses present.[39] The predominance of glutamatergic inputs to the GnRH neuron proximal dendrite may be compatible with long-standing[13] and more recent[14] evidence for an important role of glutamate transmission in the generation of the LH surge.

For the most part, the combined density of glutamatergic and GABAergic synapses approximates the total density of synaptophysin synapses. However, there may be up to 25% of synapses on the soma and initial proximal dendrite that use neither amino acid transmitter. Large scale gene profiling of individual neurons indicates

that all forebrain neurons, including those in the hypothalamus, are either glutamatergic or GABAergic.[40] As such, the few non-GABA, non-glutamate synapses identified on the soma and proximal dendrite may represent technical false negatives or rare inputs that do not use amino acid transmitters.

Evidence for synaptic plasticity at the GnRH neuron cell body and proximal dendrite in relation to the LH surge is inconsistent and, very likely, dependent on the animal model used. Electrophysiological studies using an ovariectomised, oestrogen-treated, daily cycling animal model have clearly demonstrated changes in $GABA_A$ receptor signalling at the GnRH neuron at the time of the surge.[15] However, these same changes were not identified when using a more conventional ovariectomised, oestrogen-treated model or pro-oestrous mice.[17,18] In terms of morphology, the most striking observation has been an increase in cell body and proximal dendrite spine density in surging cFos-positive GnRH neurons in conventional ovariectomised, oestrogen-treated mice.[20] However, later studies in the same mouse model were unable to document any changes in the numbers of synaptophysin appositions detected on surging GnRH neurons; the only difference was in VGAT appositions on the cell body of non-surging GnRH neurons.[21] Thus, there appears to be a curious and presently unexplained disassociation between changes in spine density and synaptic density on GnRH neuron proximal dendrites.[41] It would be of great interest to be able to examine synaptic plasticity across time in individual surging GnRH neurons, but this is not yet technically feasible.

Mice killed just prior to the onset of the pro-oestrous LH surge and at the same time on dioestrus were found here to have equal densities of synaptophysin, VGAT and VGLUT2 synapses on the cell body and proximal dendrite of preoptic area GnRH neurons. These results are very similar to those observed in ovariectomised, oestrogen-treated mice killed at the peak of the LH surge.[21] This suggests that neither the pro-oestrous, nor ovariectomised, oestrogen-evoked LH surge is associated with morphological changes in GABAergic or glutamatergic inputs to the GnRH neuron. This is consistent with the electrophysiological findings and, taken together, this indicates a lack of any robust synaptic plasticity at the GnRH neuron cell body and proximal dendrite immediately prior to or during the pro-oestrous GnRH/LH surge in mice.

Although synapse density may not change, it nevertheless remains likely that presynaptic transmitter release and postsynaptic receptor dynamics and at the GnRH neuron are altered at the time of the surge. For example, the subunit composition of AMPA receptors expressed by GnRH neurons has been reported to change at the time of the LH surge in rats.[16] The primary driver of the abrupt increase in GnRH secretion at the surge is considered to arise from presynaptic changes in electrical transmission driven by ESR1-modulated primary afferents. Precisely which combination of neurochemical inputs is required for GnRH neuron activation remains unclear. Although much evidence supports an important role for RP3V kisspeptin neurons,[42] a recent study generating an approximately 60% knockdown of ESR1 in RP3V kisspeptin neurons found only blunted LH surges and no effect on oestrous cyclicity.[12] A similar situation exists for GABA; despite $GABA_A$ receptor transmission being very important for GnRH neuron firing in vivo,[43] a 90% knockdown in GnRH neuron $GABA_A$ receptor expression had no effect on the LH surge mechanism[44] and a functional role for RP3V GABA neuron transmission in surge generation has not been identified.[11] At present, the ability to examine kisspeptin, GABAergic or glutamatergic transmission specifically at the GnRH neuron in vivo remains a significant technical challenge.

In summary, we have used ExM to assess the distribution of synapses on proximal elements of the GnRH neuron. We find that a "hot-spot" of excitatory GABAergic and glutamatergic innervation occurs 15-45 μm down the proximal dendrite with very few synapses on the cell body or distal to this region. No changes in the density of all synapses or GABAergic or glutamatergic synapses were found when comparing dioestrous and pro-oestrous mice. This suggests an absence of significant synaptic plasticity at the soma and dendrite of the GnRH neuron prior to the onset of GnRH surge in mice.

ACKNOWLEDGEMENTS

This work was supported by the New Zealand Health Research Council and Wellcome Trust.

AUTHOR CONTRIBUTIONS

Shel Hwa-Yeo: Formal analysis; Investigation; Methodology; Writing – original draft; Writing – review & editing. **Michel Herde:** Methodology. **Allan E Herbison:** Conceptualisation; Funding acquisition; Resources; Supervision; Writing – original draft; Writing-review & editing.

PEER REVIEW

The peer review history for this article is available at https://publons.com/publon/10.1111/jne.13021.

ORCID

Shel-Hwa Yeo https://orcid.org/0000-0002-0960-1799
Michel K. Herde https://orcid.org/0000-0002-2324-2083
Allan E. Herbison https://orcid.org/0000-0002-9615-3022

REFERENCES

1. Herbison AE. A simple model of estrous cycle negative and positive feedback regulation of GnRH secretion. *Front Neuroendocrinol*. 2020;57: 100837.
2. Plant TM. A comparison of the neuroendocrine mechanisms underlying the initiation of the preovulatory LH surge in the human, Old World monkey and rodent. *Front Neuroendocrinol*. 2012;33(2):160-168.
3. Christian CA, Moenter SM. The neurobiology of preovulatory and estradiol-induced gonadotropin-releasing hormone surges. *Endocr Rev*. 2010;31(4):544-577.
4. Herbison AE. In: Plant TM, Zeleznik AJ, eds. *Physiology of the adult GnRH neuronal network, in Knobil and Neill's Physiology of Reproduction*. Academic Press; 2015:399-467.
5. Goodman RL. In: Plant TM, Zeleznik AJ, eds. *Neuroendocrine control of goandotropin secretion: Comparative aspects, in Knobil and Neill's Physiology of Reproduction*. Academic Press; 2015:1537-1574.
6. Glidewell-Kenney C, et al. Nonclassical estrogen receptor alpha signaling mediates negative feedback in the female mouse reproductive axis. *Proc Natl Acad Sci USA*. 2007;104(19):8173-8177.

7. Wintermantel TM, Campbell RE, Porteous R, et al. Definition of estrogen receptor pathway critical for estrogen positive feedback to gonadotropin-releasing hormone neurons and fertility. *Neuron*. 2006;52(2):271-280.
8. Porteous R, Herbison AE. Genetic deletion of Esr1 in the mouse preoptic area disrupts the LH surge and estrous cyclicity. *Endocrinology*. 2019;160(8):1821-1829.
9. Hoffman GE, Smith MS, Verbalis JG. c-Fos and related immediate early gene products as markers of activity in neuroendocrine systems. *Front Neuroendocrinol*. 1993;14:173-213.
10. Wang L, Guo W, Shen X, et al. Different dendritic domains of the GnRH neuron underlie the pulse and surge modes of GnRH secretion in female mice. *Elife*. 2020;9:e56945.
11. Piet R, Kalil B, McLennan T, et al. Dominant neuropeptide cotransmission in Kisspeptin-GABA Regulation of GnRH neuron firing driving ovulation. *J Neurosci*. 2018;38(28):6310-6322.
12. Wang L, Vanacker C, Burger LL, et al. Genetic dissection of the different roles of hypothalamic kisspeptin neurons in regulating female reproduction. *Elife*. 2019;8:e43999.
13. Brann DW. Glutamate: a major excitatory transmitter in neuroendocrine regulation. *Neuroendocrinology*. 1995;61:213-225.
14. Cheong RY, Czieselsky K, Porteous R, et al. Expression of ESR1 in glutamatergic and GABAergic neurons is essential for normal puberty onset, estrogen feedback, and fertility in female mice. *J Neurosci*. 2015;35(43):14533-14543.
15. Christian CA, Moenter SM. Estradiol induces diurnal shifts in GABA transmission to gonadotropin-releasing hormone neurons to provide a neural signal for ovulation. *J Neurosci*. 2007;27(8):1913-1921.
16. Tada H, Kuroki Y, Funabashi T, et al. Phasic synaptic incorporation of GluR2-lacking AMPA receptors at gonadotropin-releasing hormone neurons is involved in the generation of the luteinizing hormone surge in female rats. *Neuroscience*. 2013;248:664-669.
17. Liu X, Porteous R, Herbison AE. Dynamics of GnRH neuron ionotropic GABA and glutamate synaptic receptors are unchanged during estrogen positive and negative feedback in female mice. *eNeuro*. 2017;4(5):ENEURO.0259-17.2017.
18. Adams C, Chen X, Moenter SM. Changes changes in GABAergic transmission to and intrinsic excitability of gonadotropin-releasing hormone (GnRH) neurons during the estrous cycle in mice. *eNeuro*. 2018;5(5):ENEURO.0171-18.2018.
19. Sheppard PAS, Choleris E, Galea LAM. Structural plasticity of the hippocampus in response to estrogens in female rodents. *Mol Brain*. 2019;12(1):22.
20. Chan H, Prescott M, Ong Z, et al. Dendritic spine plasticity in gonadatropin-releasing hormone (GnRH) neurons activated at the time of the preovulatory surge. *Endocrinology*. 2011;152(12):4906-4914.
21. Moore AM, Abbott G, Mair J, et al. Mapping GABA and glutamate inputs to gonadotrophin-releasing hormone neurons in male and female mice. *J Neuroendocrinol*. 2018;30(12):e12657.
22. Wassie AT, Zhao Y, Boyden ES. Expansion microscopy: principles and uses in biological research. *Nat Methods*. 2019;16(1):33-41.
23. Spergel DJ, et al. GABA-and glutamate-activated channels in green fluorescent protein-tagged gonadotropin-releasing hormone neuron in transgenic mice. *J Neurosci*. 1999;19(6):2037-2050.
24. Czieselsky K, Prescott M, Porteous R, et al. Pulse and surge profiles of luteinizing hormone secretion in the mouse. *Endocrinology*. 2016;157(12):4794-4802.
25. Martens H, Weston MC, Boulland J-L, et al. Unique luminal localization of VGAT-C terminus allows for selective labeling of active cortical GABAergic synapses. *J Neurosci*. 2008;28(49):13125-13131.
26. Mueller NK, Di S, Paden CM, et al. Activity-dependent modulation of neurotransmitter innervation to vasopressin neurons of the supraoptic nucleus. *Endocrinology*. 2005;146(1):348-354.
27. Schneider Gasser EM, Straub CJ, Panzanelli P, et al. Immunofluorescence in brain sections: simultaneous detection of presynaptic and postsynaptic proteins in identified neurons. *Nat Protoc*. 2006;1(4):1887-1897.
28. Wallrafen R, Dresbach T. The presynaptic protein mover is differentially expressed across brain areas and synapse types. *Front Neuroanat*. 2018;12:58.
29. Peng H, Bria A, Zhou Z, et al. Extensible visualization and analysis for multidimensional images using Vaa3D. *Nat Protoc*. 2014;9(1):193-208.
30. Flak JN, Ostrander MM, Tasker JG, et al. Chronic stress-induced neurotransmitter plasticity in the PVN. *J Comp Neurol*. 2009;517(2):156-165.
31. Clifton NE, Trent S, Thomas KL, et al. Regulation and function of activity-dependent homer in synaptic plasticity. *Mol Neuropsychiatry*. 2019;5(3):147-161.
32. Kasaragod VB, Schindelin H. Structure of heteropentameric GABAA receptors and receptor-anchoring properties of gephyrin. *Front Mol Neurosci*. 2019;12:191.
33. Kasthuri N, Hayworth KJ, Berger DR, et al. Saturated reconstruction of a volume of neocortex. *Cell*. 2015;162(3):648-661.
34. Campbell RE, Han SK, Herbison AE. Biocytin filling of adult gonadotropin-releasing hormone neurons in situ reveals extensive, spiny, dendritic processes. *Endocrinology*. 2005;146(3):1163-1169.
35. Silverman A, Livne I, Witkin JW. The gonadotrophin-releasing hormone (GnRH), neuronal systems: immunocytochemistry and in situ hybridization. In Knobil E, Neill JD, eds. *The Physiology of Reproduction* (pp. 1683-1706). 1994, New York.
36. Iremonger KJ, Herbison AE. Initiation and propagation of action potentials in gonadotropin-releasing hormone neuron dendrites. *J Neurosci*. 2012;32(1):151-158.
37. Herde MK, Herbison AE. Morphological characterization of the action potential initiation segment in GnRH neuron dendrites and axons of male mice. *Endocrinology*. 2015;156(11):4174-4186.
38. Moenter SM. Identified GnRH neuron electrophysiology: a decade of study. *Brain Res*. 2010;1364:10-24.
39. Kaeser PS, Regehr WG. Molecular mechanisms for synchronous, asynchronous, and spontaneous neurotransmitter release. *Annu Rev Physiol*. 2014;76:333-363.
40. Chen R, Wu X, Jiang L, et al. Single-cell RNA-Seq reveals hypothalamic cell diversity. *Cell Rep*. 2017;18(13):3227-3241.
41. Rochefort NL, Konnerth A. Dendritic spines: from structure to in vivo function. *EMBO Rep*. 2012;13(8):699-708.
42. Herbison AE. Control of puberty onset and fertility by gonadotropin-releasing hormone neurons. *Nat Rev Endocrinol*. 2016;12(8):452-466.
43. Constantin S, Iremonger KJ, Herbison AE. In vivo recordings of GnRH neuron firing reveal heterogeneity and dependence upon GABAA receptor signaling. *J Neurosci*. 2013;33(22):9394-9401.
44. Lee K, Porteous R, Campbell RE, et al. Knockdown of GABA(A) receptor signaling in GnRH neurons has minimal effects upon fertility. *Endocrinology*. 2010;151(9):4428-4436.

How to cite this article: Yeo S-H, Herde MK, Herbison AE. Morphological assessment of GABA and glutamate inputs to GnRH neurons in intact female mice using expansion microscopy. *J Neuroendocrinol*. 2021;00:e13021. https://doi.org/10.1111/jne.13021